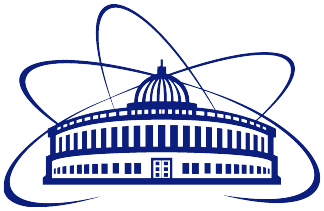

JOINT INSTITUTE FOR NUCLEAR RESEARCH
Veksler and Baldin laboratory of High Energy Physics

FINAL REPORT ON THE START PROGRAMME

Analysis of the Two-Pion Correlation Function at the BM@N and MPD Experiments

Supervisor:
Dr. Ivonne Alicia Maldonado Cervantes

Student:
Santiago Bernal Langarica, Mexico
Nuclear Sciences Institute,
National Autonomous University of Mexico

Participation period:
July 3rd – August 25th,
Summer session, 2023

Dubna, 2023

Abstract

The study of the matter that forms after the collision of relativistic heavy-ion collisions is an active research field. One of its main branches is femtoscopy, the characterization of the spatiotemporal source that emits the particles that can be detected. To achieve this goal, one of the most common techniques is the study of the two-pion correlation function, which is an observable quantity that easily allows the determination of the source size. In this work, the two-pion correlation function was obtained for the BM@N argon run at 3.2 GeV data, as well as for the request 31 of MPD Monte Carlo data, which consists of bismuth + bismuth collisions at 9.2 GeV.

Contents

Acknowledges

I would like to the express my gratitude to the Joint Institute for Nuclear Research and the Veskler and Baldin Laboratory for High Energy Physics for providing me the opportunity and the funding to work on this project and to be at the Institute for the duration of the START programme. In that same sense, I would like to thank the START team office for everything that they did.

On the academic realm, I would like to thank my supervisor, Dr. Ivonne Maldonado, for all the support and teachings during this internship, as well as to Dr. Nelli Pukhaeva, Dr. Alexey Aparin and to Dr. Vasilii Plotnikov, for their useful and fruitful comments, suggestions, lectures and for providing me the BM@N data to analyse.

I would also like to thank my office co-workers, for their quick answers to all the small questions that I had during the work hours.

Thank you very much to all!

Chapter 1

Introduction

The Standard Model of Particle Physics is the collection of quantum field theories that best describe the experimental and some of the phenomenological results that humanity has obtained about the fundamental interactions and particles that compose our known universe. One of such theories is the theory of the strong interaction called Quantum Chromodynamics (QCD), a Yang–Mills SU(3) theory that describes, at the most fundamental level, the interactions of fermions (quarks) and bosons (gluons). Due to the fact that the strong coupling constant of QCD has a large value, perturbative calculations are not always valid, and therefore, the predictions of this theory are still unknown under certain regimes.

As it was previously stated, QCD describes the interactions of quarks (grouped into three generations, with two flavours per generation), and gluons (which come in eight colours). As a consequence of this, the QCD beta function, which describes the rate of change of the coupling constant, is negative. This implies that, at higher energies, the coupling constant decreases, and allows the deconfinement of quarks and gluons in at least one kind of state called the quark gluon plasma (QGP). This is usually referred to as the asymptotic freedom property of QCD.

The exploration of the phases of matter at different energetic regimes, such as temperature, baryonic chemical potential, isospin chemical potential, magnetic field, among others is called the QCD phase diagram. Different physical scenarios allow us to study these different regimes, for example, the high temperature and small baryonic chemical potential regime corresponds to the early universe; the low temperature, large baryonic chemical potential and non-zero isospin chemical potential regime, corresponds to the matter state at the core of neutron stars; while the not-so-high temperature and baryonic chemical potential corresponds to the relativistic heavy–ion collision experiments that are made on laboratories.

This makes this last regime of great interest, since it is the only of the said regimes that is experimentally accessible on Earth, and hence, allows the scientific community to compare experimental results with theoretical predictions. To make this comparison, one needs to characterise the collision in terms of temperature and chemical potential, as well as the geometry and size of the interaction region where the particles that could

be detected in an experiment, are being produced. This last aspect has been addressed with several techniques over the last years, one of particular relevance is based on the interferometric technique developed by Hanbury-Brown and Twiss in the context of the determination of the source size of stellar objects by taking into account the interference of two bosonic particles (such as photons) that are being chaotically emitted. The spatio-temporal study of the emitting source after the collision of relativistic heavy ions receives the name of femtoscopy.

In this work, the techniques of femtoscopy were applied to data sets of BM@N and MPD experiments, which are located at the Nucleotron-based Ion Collider fAcility (NICA) complex of the Joint Institute for Nuclear Research (JINR) in Dubna, Russia. This work is organized as follows: In Chapter 1, the basic ideas of identical particle femtoscopy are presented. In Chapter 2, the work done with BM@N data is presented. In Chapter 3, the work done with MPD data is presented. Finally, in Chapter 4, the conclusions of this work are presented.

1.1 The two-particle correlation function in position space

In the second half of the 1950's, Hanbury-Brown and Twiss performed an experiment in which they measured the probability amplitude of detecting two photons, coming from the same coherent source, in different space points at neighbouring time. The experiment reveal, both the bosonic nature of photons (which is contained within the superposition principle for classical electromagnetism) and a typical quantum effect that occurs in bosonic gases [1]. Their main results are, first of all, the tendency of photons to group together, as a consequence of the superposition principle and secondly, that the measured correlated intensity has a part that is independent of the size of the source plus a part that depends on the size of the source, thus allowing to determine the size of the source by measuring the correlation intensity of photons[1]. This technique has been used in the context of astrophysics, for the analysis of the spacial size of stars, galaxies, among others, as well as in the context of relativistic heavy-ion collisions to determine the spatial extent of the source, which is the main objective of this work.

Following Ref. [1], assuming a dilute system of indistinguishable and non-interacting bosons, consider an N-particle state on the form

$$|\psi\rangle = \frac{1}{\mathcal{N}} \prod_{\mathbf{p}_i} \left[\hat{a}^\dagger(\mathbf{p}_i)\right]^{N(\mathbf{p}_i)} |0\rangle \,, \tag{1.1}$$

where $\mathcal{N}$ represents a normalization factor and N is the occupation number of the state, $\hat{a}^\dagger$ and $\hat{a}$ are a creation and annihilation operators that act as

$$\hat{a}^\dagger(\mathbf{p}) \,|\psi\rangle = \sqrt{N(\mathbf{p})+1} \left|\psi^{[N(\mathbf{p}+1]}\right\rangle \tag{1.2}$$

$$\hat{a}(\mathbf{p}) \,|\psi\rangle = \sqrt{N(\mathbf{p})} \left|\psi^{[N(\mathbf{p}-1]}\right\rangle . \tag{1.3}$$

[1] Details of this will be provided later throughout this chapter.

If we define the field operator

$$\hat{\varphi}(\mathbf{r}) = \int \frac{d^3p}{(2\pi)^3} e^{i\mathbf{p}\cdot\mathbf{r}} \hat{a}(\mathbf{p}), \tag{1.4}$$

then, the particle number density is given by

$$\langle\psi|\, \hat{\varphi}^\dagger(\mathbf{r})\hat{\varphi}(\mathbf{r})\, |\psi\rangle = \int \frac{d^3p}{(2\pi)^3} N(\mathbf{p}) = N. \tag{1.5}$$

Now, the probability amplitude of finding a particle at $\mathbf{r}'$ and another one at the same time but at the different position $\mathbf{r}$ is given by the expectation value of

$$\langle\psi|\, \hat{\varphi}^\dagger(\mathbf{r})\hat{\varphi}^\dagger(\mathbf{r}')\hat{\varphi}(\mathbf{r}')\hat{\varphi}(\mathbf{r})\, |\psi\rangle\,, \tag{1.6}$$

which leads to the matrix element

$$\langle\psi|\, \hat{a}^\dagger(\mathbf{p})\hat{a}^\dagger(\mathbf{q})\hat{a}(\mathbf{q}')\hat{a}(\mathbf{p}')\, |\psi\rangle\,. \tag{1.7}$$

This matrix element is only non-vanishing if $\mathbf{p} = \mathbf{q}$. It can be shown (see Ref. [1]) that

$$\begin{aligned}\langle\psi|\, \hat{a}^\dagger(\mathbf{p})\hat{a}^\dagger(\mathbf{q})\hat{a}(\mathbf{q}')\hat{a}(\mathbf{p}')\, |\psi\rangle = (2\pi)^6 \left[\delta(\mathbf{p}-\mathbf{p}')\delta(\mathbf{q}-\mathbf{q}') + \delta(\mathbf{p}-\mathbf{q}')\delta(\mathbf{q}-\mathbf{p}')\right] N(\mathbf{p})N(\mathbf{q}) \\ - (2\pi)^9 \delta(\mathbf{p}-\mathbf{q})\delta(\mathbf{p}-\mathbf{p}')\delta(\mathbf{q}-\mathbf{q}')N(\mathbf{p})\left(N(\mathbf{p})+1\right),\end{aligned} \tag{1.8}$$

and hence

$$\langle\psi|\, \hat{\varphi}^\dagger(\mathbf{r})\hat{\varphi}^\dagger(\mathbf{r}')\hat{\varphi}(\mathbf{r}')\hat{\varphi}(\mathbf{r})\, |\psi\rangle = N^2 + \left|\int \frac{d^3p}{(2\pi)^3} e^{i\mathbf{p}\cdot(\mathbf{r}-\mathbf{r}')} N(\mathbf{p})\right|^2 - \left|\int \frac{d^3p}{(2\pi)^3} N(\mathbf{p})\left(N(\mathbf{p}+1)\right)\right|^2. \tag{1.9}$$

Notice that the third term in Eq. (1.9) is independent of the position and by dimensional analysis, is inversely proportional to the volume where the particles are contained. Thus, for sufficiently large volumes, the contribution of this term is smaller than that of the other terms. The two-particle correlation function is defined as

$$C_2(\mathbf{r}-\mathbf{r}')N^2 = \langle\psi|\, \hat{\varphi}^\dagger(\mathbf{r})\hat{\varphi}^\dagger(\mathbf{r}')\hat{\varphi}(\mathbf{r}')\hat{\varphi}(\mathbf{r})\, |\psi\rangle\,, \tag{1.10}$$

viz., the correlation function, for sufficiently large volumes takes the approximate form

$$C_2(\mathbf{r}-\mathbf{r}') = 1 + \frac{1}{N^2}\left|\int \frac{d^3p}{(2\pi)^3} e^{i\mathbf{p}\cdot(\mathbf{r}-\mathbf{r}')} N(\mathbf{p})\right|^2. \tag{1.11}$$

From this equation, it can be seen that the correlation function has a minimum value of 1 and a maximum value of 2 for $\mathbf{r} = \mathbf{r}'$. Additionally, if one assumes that the average particle number density is characterized by a Gaussian momentum distribution, such as

$$N(\mathbf{p}) = \alpha e^{\beta(\mathbf{p}-\mathbf{p}_0)^2/2,} \tag{1.12}$$

then, the two-particle correlation function takes the form

$$C_2(\mathbf{r}-\mathbf{r}') = 1 + \exp\Big(-|\mathbf{r}-\mathbf{r}'|^2/\sqrt{\beta}\Big). \tag{1.13}$$

1.2 The two-particle correlation function in momentum space

Following Ref. [2], assuming a dilute system of indistinguishable and non-interacting bosons, the occupation number of a state with a set of quantum numbers λ, is given by

$$N_\lambda = \frac{1}{\exp(E_\lambda - \mu)/T - 1}, \tag{1.14}$$

where E_λ is the energy of the state, μ is the chemical potential associated with the particle number density[2] and T is the system temperature. Given that the wave-function of the particles in momentum space, ψ_λ, is properly normalized, then it is possible to define the single-particle momentum distribution as

$$P_1(\mathbf{p}) \equiv \frac{\mathrm{d}^3 N}{\mathrm{d}p^3} = \frac{1}{(2\pi)^3} \sum_\lambda 2E_\lambda N_\lambda \psi^*_\lambda(\mathbf{p})\psi_\lambda(\mathbf{p}). \tag{1.15}$$

The total number of particles can be shown to be obtained from

$$N = \sum_\lambda \frac{1}{\exp(E_\lambda - \mu)/T - 1}. \tag{1.16}$$

For a totally chaotic particle source, the two-particle momentum distribution is given by

$$P_2(\mathbf{p}_1, \mathbf{p}_2) \equiv \frac{\mathrm{d}^6 N}{\mathrm{d}p_1^3\, \mathrm{d}p_2^3} = P_1(\mathbf{p}_1)P_1(\mathbf{p}_2) + \left| \frac{1}{(2\pi)^3} \sum_\lambda 2E_\lambda N_\lambda \psi^*_\lambda(\mathbf{p}_1)\psi_\lambda(\mathbf{p}_2) \right|^2, \tag{1.17}$$

from where the two-particle correlation function C_2 is expressed in terms of the single- and two-particle momentum distributions as

$$C_2(\mathbf{p}_1, \mathbf{p}_2) = \frac{P_2(\mathbf{p}_1, \mathbf{p}_2)}{P_1(\mathbf{p}_1)P_1(\mathbf{p}_2)} = 1 + \frac{\left| \sum_\lambda E_\lambda N_\lambda \psi^*_\lambda(\mathbf{p}_1)\psi_\lambda(\mathbf{p}_2) \right|^2}{\sum_\lambda E_\lambda N_\lambda \left|\psi(\mathbf{p}_1)\right|^2 \sum_\lambda E_\lambda N_\lambda \left|\psi(\mathbf{p}_2)\right|^2}. \tag{1.18}$$

When the particle source is not totally chaotic, which happens when the fraction of particles in the ground state is not negligible, its contribution to the correlation function must be separated as

$$\begin{aligned} C_2(\mathbf{p}_1, \mathbf{p}_2) = 1 &+ \frac{\left|\sum_\lambda E_\lambda N_\lambda \psi^*_\lambda(\mathbf{p}_1)\psi_\lambda(\mathbf{p}_2)\right|^2}{\sum_\lambda E_\lambda N_\lambda \left|\psi(\mathbf{p}_1)\right|^2 \sum_\lambda E_\lambda N_\lambda \left|\psi(\mathbf{p}_2)\right|^2} \\ &+ \frac{\left|E_{\lambda_0} N_{\lambda_0} \psi^*_{\lambda_0}(\mathbf{p}_1)\psi_{\lambda_0}(\mathbf{p}_2)\right|^2}{\sum_\lambda E_\lambda N_\lambda \left|\psi(\mathbf{p}_1)\right|^2 \sum_\lambda E_\lambda N_\lambda \left|\psi(\mathbf{p}_2)\right|^2}, \end{aligned} \tag{1.19}$$

[2] This chemical potential corresponds to an effective description of the (in average) approximately conserved number of particles

where λ_0 represents the set of quantum numbers corresponding to the ground state. Notice that when particles coming from the ground state are treated separately from the ones coming from excited states, the correlation function fails to reach its maximum possible value $C_2(q=0)_{\max} = 2$ as the ground state occupation number increases. This happens since for $\mathbf{q} = \mathbf{p}_1 - \mathbf{p}_2 = 0$, the numerator and the denominator of the second and third terms on the right-hand side of Eq. (1.19) are no longer equal, as they were in Eq. (1.18) for the case of a totally chaotic source.

Notice that the two-particle correlation function C_2 depends on the six kinematical variables corresponding to the two-particle momenta as well as parametrically on μ, T and other factors that affect the system, such as its finite volume, magnetic field, expansion velocity, among others. The properties of the correlation function can be more easily studied by setting particular configurations of these kinematical variables. Usually, the correlation function is reported as a function of the magnitude of the momentum difference $q = |\mathbf{p}_1 - \mathbf{p}_2|$, and for fixed values of the average momentum $K = \frac{1}{2}(p_1 + p_2)$.

1.3 The two-particle correlation function in experiments

When one tries to compute the two-particle correlation function from Monte Carlo or real experimental data, the previous definitions are rarely used. Instead, it is usually more easy to compute it from

$$C_2(q, K) = \frac{S(q, K)}{B(q, K)}, \tag{1.20}$$

where S is the signal distribution and B is the background distribution [3]. The idea behind this form of the correlation function is that S and B are (ideally) similar, except for the presence of the correlations in S that should not exist in B, hence, by taking the ratio, only the correlations should remain. Now, the question that arises is how to construct the S and B distributions? The S distribution can be constructed by obtaining the relative and average momentum distribution of pairs of particles that are produced in the same event, while the B distribution can be constructed by obtaining the relative and average momentum distributions of pairs of particles that are produced in different events. This technique is referred as event mixing. One important thing to note is that the events used for the construction of B must have similar properties: they must have similar primary vertex, centrality, orientation of transverse plane and come from events close in time, since detector acceptance can vary with time. Other techniques to compute B can be found in Ref. [3].

To make sure that, at high relative momentum, the two-particle correlation function has a value of unity, a normalization factor can be included in Eq. (1.20) as [4]

$$C_2(q, K) = \frac{S(q, K)}{B(q, K)} \cdot \frac{\int_{q_1}^{q_2} B(q, K) dq}{\int_{q_1}^{q_2} S(q, K) dq}, \tag{1.21}$$

where $[q_1, q_2]$ is a large-q range where quantum statistical effects no longer affect the correlation function.

Chapter 2

Two-particle correlation function from BM@N data

2.1 Description of BM@N

The Barionic Matter at Nucleotron (BM@N) is one of the main research facilities at the NICA complex is a fixed target experiment that collides different kind of heavy-ion beams with different targets.

The BM@N experiment main purpose is to study baryonic matter, particularly the production of strange matter in heavy-ion collisions at beam energies between 2 and 6 GeV. The first physics results of the experiment were presented in 2019.

The detector setup is shown in Figure 2.1 and comprises various components, including several triggers, silicon tracking systems, silicon beam profilers, time-of-flight detectors (ToF), electromagnetic and hadron calorimeters, which allow to measure the trajectories, momenta and energy loss of the particles produced in the collisions. Of particular interest to this work are the ToF detectors, that measure the time taken by a charged particle to travel a known distance (usually determined by scintillator plastics), hence allowing the identification of the particle. Since the main particle identification system of the BM@N experiment is based on this detectors [5, 6], their data will be of the upmost importance for this study. However, the only available data was from the left part of the ToF400 system (see Figure 2.1).

The purpose of the study made is to obtain the two-pion correlation function from the Ar-nucleus collision data that was obtained during the commissioning phase.

2.2 Description of BM@N data

To obtain the two-pion correlation function it is important to properly identify the particles and to have good measurements of its total momentum, in each direction. Therefore, the data of ToF400 is necessary to compute the two-pion correlation function, since it is from this detector that the identification of the particles is done. However,

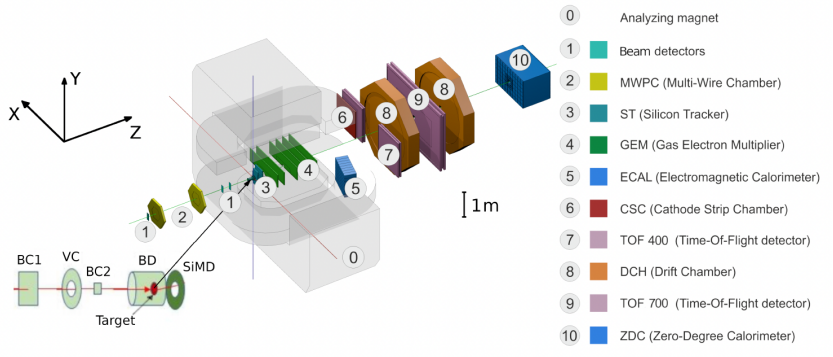

Figure 2.1: Schematic view of the BM@N setup. Figure taken from [6].

only charged particles with *hard* momenta can reach the ToF detectors, and thus, the statistics is limited.

The set of data that was used for this purpose was a subset of selected reconstructed data, with cuts on the number of hits at the Gas Electron Multiplier (GEM); on the primary vertex position; extrapolation to the Cathode Strip Chamber (CSC); number of Silicon tracker (ST) hits and number of trigger signals [5]. All of these cuts are optimized for the identification of protons, kaons and pions and are stored in the form of a ROOT data tree file, which contained data from the argon beam run, which consisted of an argon beam of energy 3.2 GeV and it only contained data from the left part of the ToF. Additionally, the particles contained a cut in their rapidity (assuming that the detected particle is a pion) of $1.5 < y_\pi < 3.2$. The complete list of the variables found on the data can be found on Table 2.1. Within all of those variables, the ones that were used for the computation of the correlation function were the squared mass; the total momentum; the rapidity, assuming that the particle is a pion; the energy, assuming that the particle is a pion; the run id; the event id; the target id; the X, Y and Z coordinates of the primary vertex.

Finally, according to Ref. [5], additional cuts must be imposed to ensure the quality of the data:

- The events must have a primary vertex Z distance to the origin within $-3.4 < |Z_{PV} - Z_0| < 1.7$ cm and a $X - Y$ distance $dca < 1$ cm
- The pions must have a total momentum $P < 0.5$ GeV
- Pions are identified by their square mass interval of $-0.09 \leq m^2 \leq 0.13$ GeV^2

It is important to notice that this cuts are satisfied by approximately 98 % of the pions present in the sample, so there are no significant difference after imposing them.

On the other hand, the multiplicity of all the charged particles is shown in Figure 2.2, where we can see that the average multiplicity is slightly above one, which means, that in almost 80 % of the events, only one particle was detected by the ToF400 and at most, on 0.00001 % of the events, seven particles were recorded. The multiplicity of pions is

Table 2.1:
List of variables found on the worked BM@N data.

Variable name	Description
m2	squared mass of the track
px	X-projection of the track momentum
py	Y-projection of the track momentum
pz	Z-projection of the track momentum
p	full track momentum
ypi	track rapidity, assuming the track is a pion
yk	track rapidity, assuming the track is a kaon
pt	transverse momentum of the track
beta	the speed of the track in units of the speed of light (c)
epi	full energy of the track, assuming the track is a pion
ek	full energy of the track, assuming the track is a kaon
nutrpv	number of tracks in the primary vertex (PV)
nurun	run id
nuev	event id in the run
nutrig	trigger id
nutarg	target id (1 - C; 2 - Al; 3 - Cu; 4 - Sn; 5 - Pb)
nubd	number of Barrel Detector (BD) trigger signals in the event
nufd	number of Forward Detector (FD) trigger signals in the event
nuvc	number of Veto Counter (VC) trigger signals in the event
xcsc	X-coordinate of the Cathode Strip Chamber (CSC) hit for the track
ycsc	Y-coordinate of the Cathode Strip Chamber (CSC) hit for the track
zcsc	Z-coordinate of the Cathode Strip Chamber (CSC) hit for the track
dxcsc	X residual for the track in the CSC
dycsc	Y residual for the track in the CSC
xtof400	X-coordinate of the ToF-400 hit for the track
ytof400	Y-coordinate of the ToF-400 hit for the track
ztof400	Z-coordinate of the ToF-400 hit for the track
dxtof400	X residual for the track in the TOF400
dytof400	Y residual for the track in the TOF400
xpv	X-coordinate of the PV in the event
ypv	Y-coordinate of the PV in the event
zpv	Z-coordinate of the PV in the event
dcax	X DCA (Distance of Closest Approach) relating to the PV
dcay	Y DCA (Distance of Closest Approach) relating to the PV
nsi	number of Si (Silicon tracker, ST) hits in the track
ngem	number of GEM hits in the track

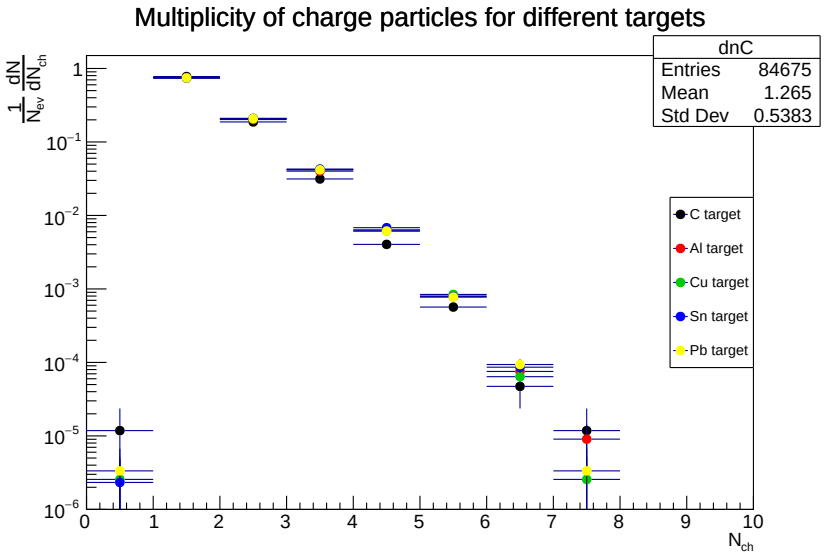

Figure 2.2: Charged particles multiplicity of the analysed BM@N data for each target.

shown in Figure 2.3, where it is evident that in over 90 % of the events, there was no pion recorded.

The transverse momentum distribution of the pions that passed the above mentioned cuts is shown in Figure 2.4, from where it can be seen that the number of pions with transverse momentum smaller than 0.3 GeV) is significantly higher than for those with transverse momentum greater than 0.4 GeV. This is due to the fact that the presented distribution is integrated over the rapidity interval.

2.3 Relative momentum distributions and two-particle correlation function

As was mentioned in Chapter 1, to compute the two-pion correlation function it is needed to obtain the relative momentum distribution for particles of the same event and for particles of different events. The construction of the former distribution is very straightforward, while, as it was also mentioned, the construction of the latter needs some additional cuts: the maximum primary vertex distance that was considered for the event mixing is of 10 cm and the events must be within the 100 closest events (this last amount is due to the values that the number of events take).

The same event relative distribution was obtained from the number of pairs that is shown in Table 2.2. As it can be seen in the said table, the amount of pairs per event is very low, even for high luminosity targets (such as aluminium), where the flux of particles is grater than for the rest of the particles. Nonetheless, for heavier targets, the multiplicity tends to be higher, so there appears to be an equilibrium between the flux of particles produced in the collision and the multiplicity, but still, the number of

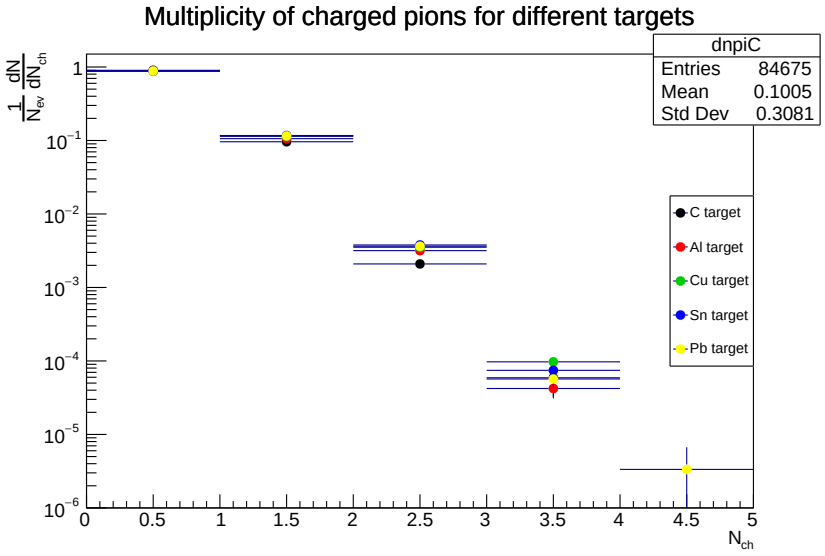

Figure 2.3: Pion multiplicity of the analysed BM@N data for each target.

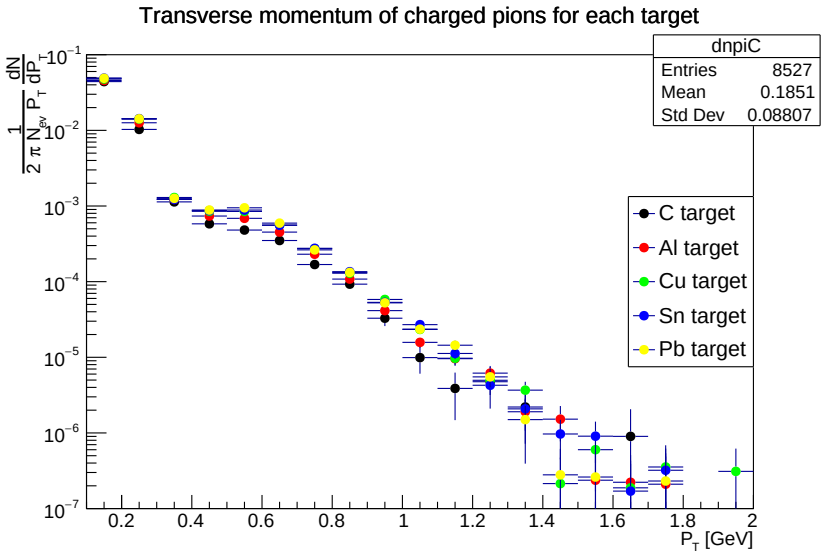

Figure 2.4: Pion transverse momentum distribution of the analysed BM@N data for each target.

Table 2.2: Multiplicity of pions and number of pairs than can be created with the available data, for each target.

	ArC ($L = 2.1\mu b^{-1}$)	ArAl ($L = 2.4\mu b^{-1}$)	ArCu ($L = 1.8\mu b^{-1}$)	ArSn ($L = 1.1\mu b^{-1}$)	ArPb ($L = 0.5\mu b^{-1}$)
Total Events	86,047	331,771	390,691	429,425	299,021
Events with 1 pion	8,139	35,183	44,632	50,180	34,472
Events with 2 pion	177	1,052	1,378	1,626	1,089
Events with 3 or more pions	4	14	38	32	18
Pairs of pions from the same event	192	1,094	1,492	1,722	1,146

pairs is small. Briefly speaking, the amount of pairs available to construct the relative momentum distribution is small, and not that different, for all the targets.

In Figures 2.5, 2.6, 2.7, 2.8 and 2.9 it is shown the obtained relative momentum distributions for the same events, in blue, and for mixed events, in red, as well as the two-pion correlation function, for each target. As it can be seen, for all the targets the two-pion correlation function is flat, which would imply that there is no correlation among the detected pions. However, this could be due to the extremely low statistics available in the data sample, as it is evidenced in Table 2.2.

2.4 How to improve the obtained results

Notice that for the highest luminosity target (ArAl), only 0.33 % of the events have multiple pions, hence it is possible to construct only approximately 1100 pairs of pions, while for the highest multiplicity target (ArPb), only 0.37 % of the events have multiple pions, hence it is possible to construct also approximately 1100 pairs of pions.

As was stated before, the data only contains the left part of the ToF400 detector, therefore if the data of the other part of the Tof400 was available, it could be possible to increase the multiplicity (and even double it) and construct more pairs, which would augment the statistics, hence making possible to possibly seeing the expected correlation

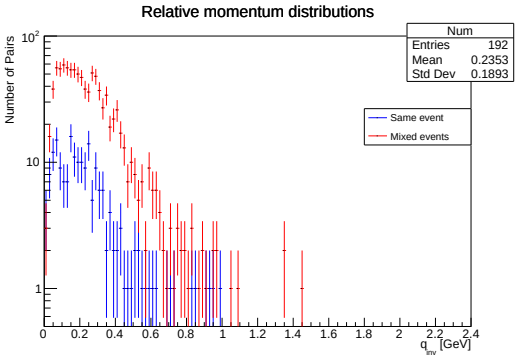

(a) Relative momentum distributions

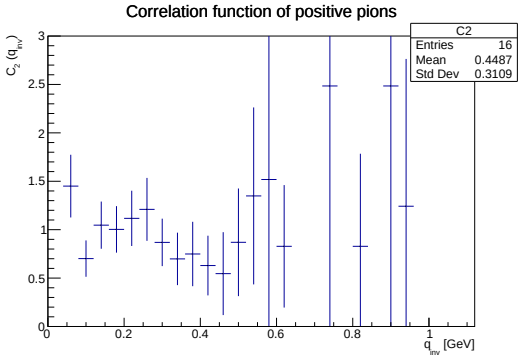

(b) Two-pion correlation function

Figure 2.5: (a) Relative momentum distributions and (b) two-pion correlation function for the carbon target.

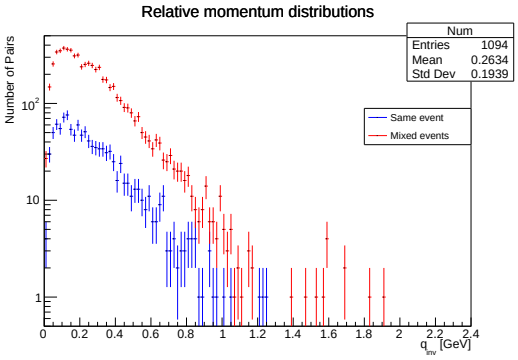

(a) Relative momentum distributions

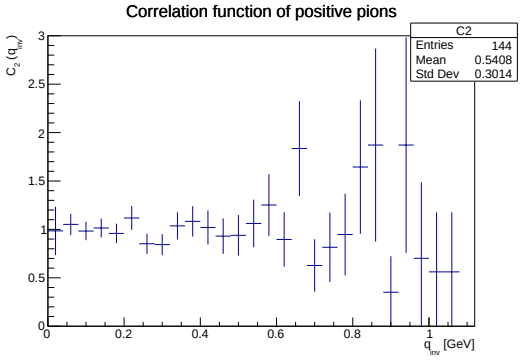

(b) Two-pion correlation function

Figure 2.6: (a) Relative momentum distributions and (b) two-pion correlation function for the aluminium target.

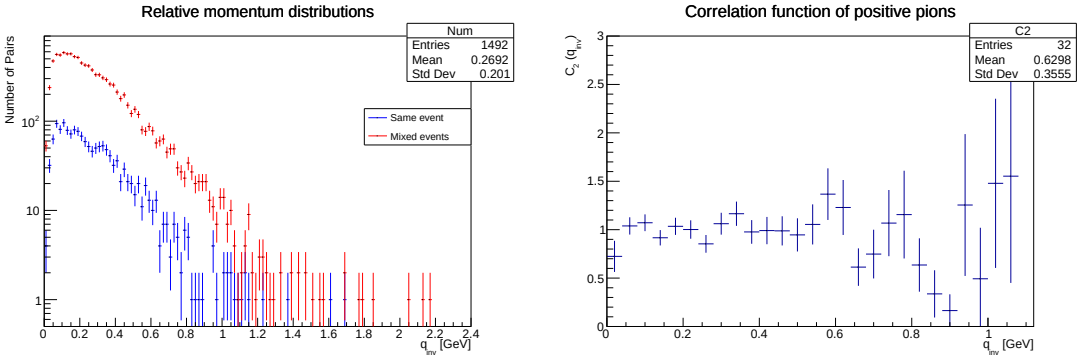

(a) Relative momentum distributions (b) Two-pion correlation function

Figure 2.7: (a) Relative momentum distributions and (b) two-pion correlation function for the copper target.

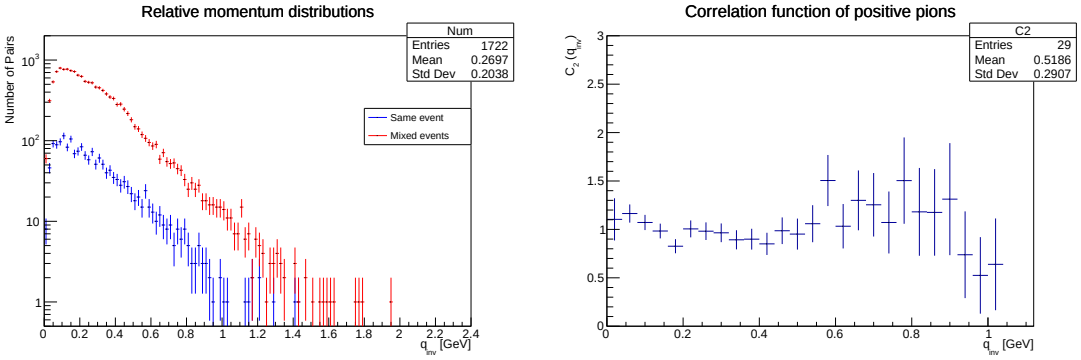

(a) Relative momentum distributions (b) Two-pion correlation function

Figure 2.8: (a) Relative momentum distributions and (b) two-pion correlation function for the tin target.

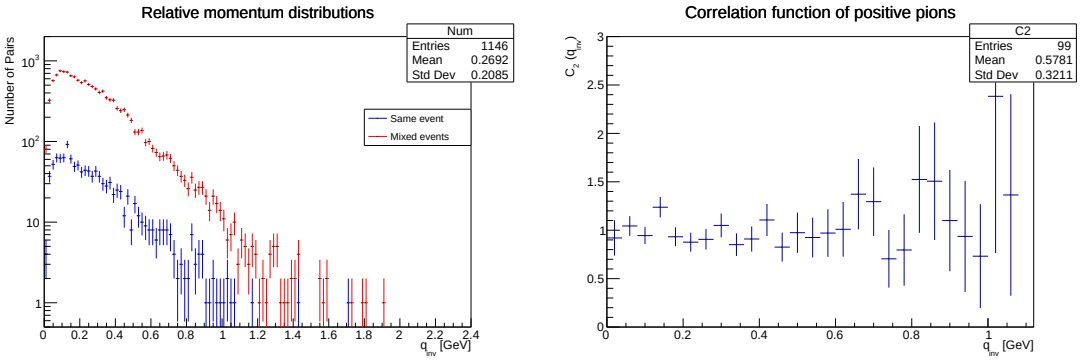

(a) Relative momentum distributions

(b) Two-pion correlation function

Figure 2.9: (a) Relative momentum distributions and (b) two-pion correlation function for the lead target.

among the charged pions. Hence, to see the effect it might be needed about ten times more pairs, which means three million events that passes the quality cuts, for each target or even less if the other Tof400 could provide data.

Chapter 3

Two-particle correlation function from MPD data

3.1 Description of MPD

The Multi Purpose Detector (MPD) is one of the major scientific project conducted at the NICA complex. It is a detector of the product of relativistic heavy-ion collisions, mostly bismuth, lead and gold, between 4 and 11 GeV.

The MPD experiment aims to investigate the behaviour of the quark gluon plasma in the region of large baryonic chemical potential, and not so high temperature. Currently, under construction at the JINR, it is expected to have its first experimental run in 2025.

The MPD detector is shown on Figure 3.1 and it consists of various subsystems, including tracking detectors, electromagnetic and hadronic calorimeters, ToF detectors, Time Projection Chamber (TPC) and the Fast Forward detector [7]. Since at the time of writing it is still a project under construction and development, only Monte Carlo and simulated data are available to work with.

The current object oriented set of tools for the physical analysis, simulation and reconstruction of the MPD experiment is the software framework called `mpdroot`. At this moment, the pure and reconstructed Monte Carlo data are produced under request and stored at the NICA cluster facility.

The purpose of the study made is to obtain the two-pion correlation function from the pure Monte Carlo data of Request 31.

3.2 MPD request 31 data

The Monte Carlo of the request 31 consists of one million minimum bias events, of bismuth + bismuth collisions at center of mass energy $\sqrt{s_{NN}} = 9.2$ GeV, simulated by the Ultrarelativistic Quantum Molecular Dynamics (UrQMD) generator and reconstructed using GEometry ANd Tracking-3 (GEANT-3) with the detector configuration for femtoscopy only. Since it is a femtoscopy purpose simulation, it contains the freeze-out

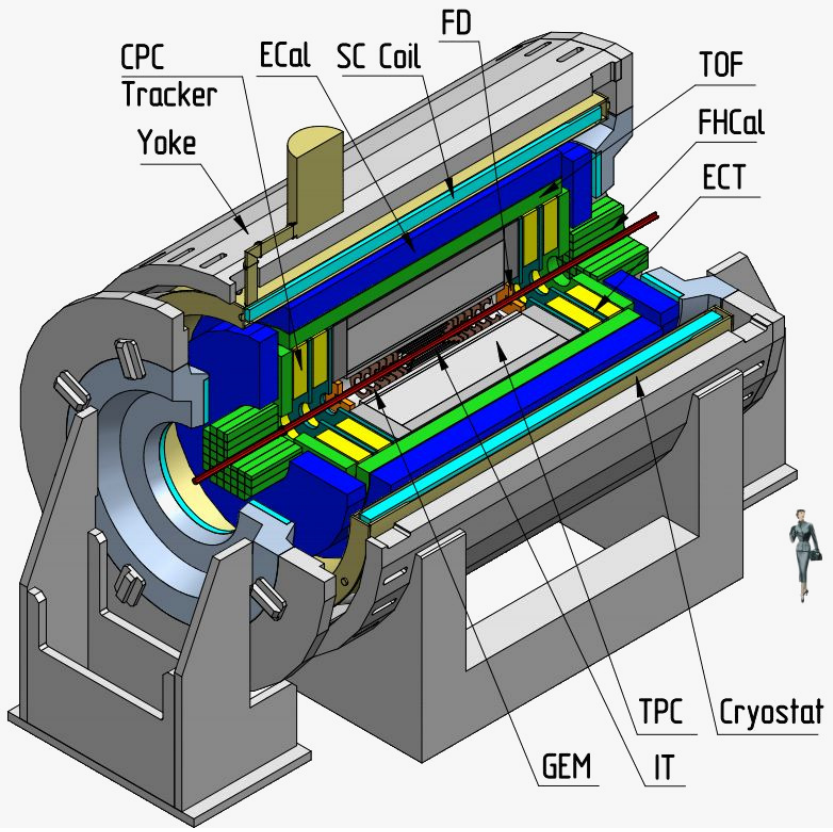

Figure 3.1: Schematic view of the MPD experiment. Figure taken from Ref. [7]

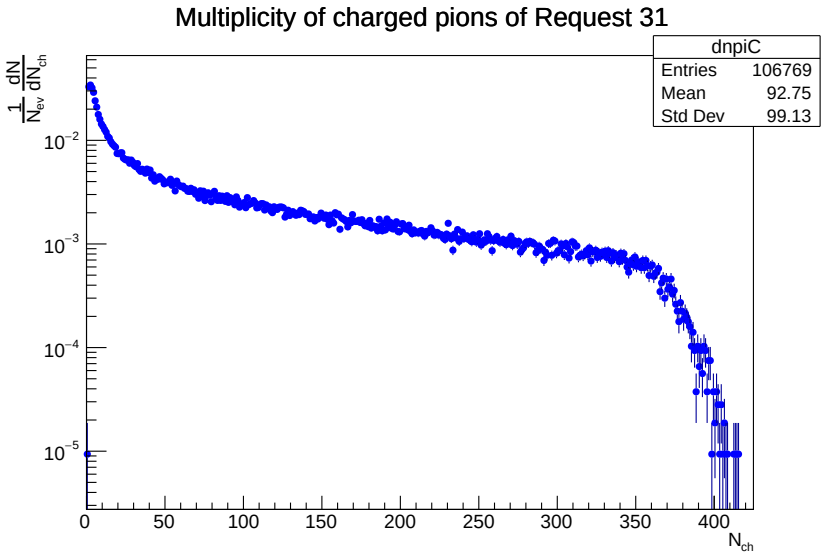

Figure 3.2: Charged pion multiplicity of the analysed MPD data.

coordinates. These coordinates are important for the adding of the correlation to non-correlated data, such as the output of UrQMD, and are not present in most of the other requests.

The files contain several kinds of data: `EventHeader`, with the event information; `MpdTpc`, with the information of the TPC detector; `TpcKalmanTrack`, with the track information; `Vertex`, with the vertex information; `FdfHit`, with the number of Fast Forward Detector hits;`TOFHit`, with the number of ToF detector hits; `TOFMatching`, with information about the reconstruction; `ZdcDigi`, with the information of the Forward Hadron Calorimeter; `MCEventHeader`, with the information of the pure Monte Carlo event; `MCTrack`, with the information of the Monte Carlo track; `GenTracks`, with the track information; and `MPDEvent`, with the reconstructed track information. However, since the goal of the computation is to obtain the correlation from pure Monte Carlo, only the global event information, such as the impact parameter and event number, as well as the `MCTrack` data were used. The relevant information of the Monte Carlo tracks, were the PdgCode, MotherId, total momentum projections, transverse momentum, energy, position and rapidity.

Following the cuts mentioned in Ref. [7], a cut on the transverse momentum of $P_T < 3$ GeV and a provisional cut on the rapidity $|\eta| < 2$ of the tracks were imposed. This cut is not very realistic, but it is imposed to achieve a better statistics, but will be improved to a more realistic value for future work. For the charged pions that passed the said cuts, their multiplicity is shown in Figure 3.2, while their transverse momentum distribution is shown in Figure 3.3.

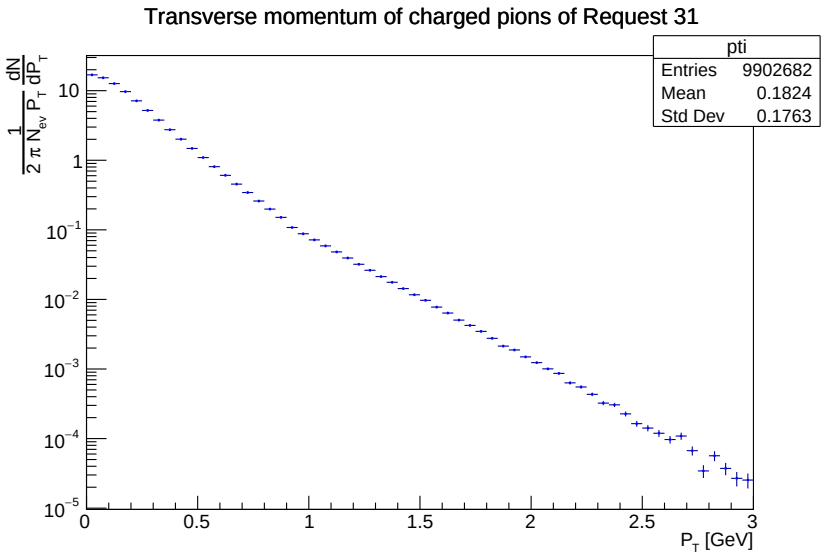

Figure 3.3: Charged pion transverse momentum of the analysed MPD data.

3.3 Relative momentum distributions and two-particle correlation function

As it has been previously stated in multiple occasions, to construct the two-pion correlation it is needed to impose some additional cuts for the event mixing technique: in this case it was considered that the events where within the next 5 events, had a maximum distance in the $X - Y$ plane of the primary vertex of 2 cm and 10 cm in the Z direction, the events must have similar impact parameter and average transverse momentum between 0.2 and 2. GeV.

In Figure 3.4, the relative momentum distributions and the two-pion correlation function for events with impact parameter $b = 0 - 2$ fm, are shown. The fit to a Gaussian function

$$C_2(q_{inv}) = 1 + \lambda \exp\left(-\left(\frac{q_{inv}R}{\hbar c}\right)^2\right), \tag{3.1}$$

where $\hbar$ is Planck's constant and c is the speed of light, and $\hbar c = 0.197327$ GeV fm. For this case the fit result was $R = 0.2358 \pm 0.0003$ fm and $\lambda = 0.9582 \pm 0.0011$.

In Figure 3.5, the relative momentum distributions and the two-pion correlation function for events with impact parameter $b = 0 - 4$ fm, are shown. The fit to a Gaussian function result was $R = 0.226 \pm 0.000$ fm and $\lambda = 0.6302 \pm 0.0004$.

In Figure 3.6, the relative momentum distributions and the two-pion correlation function for events with impact parameter $b = 7 - 14$ fm, are shown. The fit to a Gaussian function result was $R = 0.2256 \pm 0.0002$ fm and $\lambda = 0.466 \pm 0.000$.

As it is easily seen from Figures 3.4, 3.5 and 3.6, the obtained correlation function has some strange properties: to start with, for the most central collisions, the value of

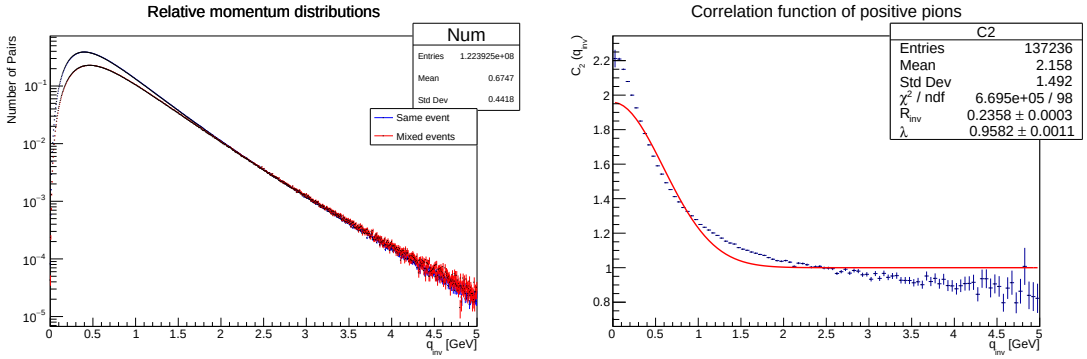

(a) Relative momentum distributions (b) Two-pion correlation function

Figure 3.4: (a) Relative momentum distributions and (b) two-pion correlation function for events with impact parameter $b = 0 - 2$ fm, computed from the MPD request 31 data.

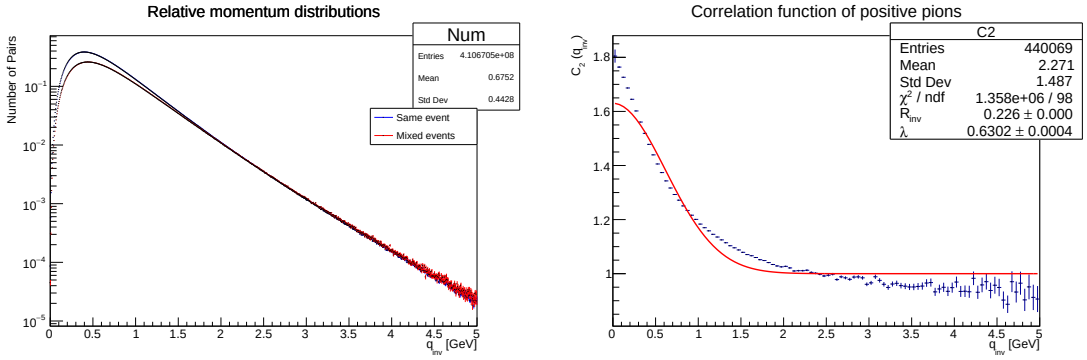

(a) Relative momentum distributions (b) Two-pion correlation function

Figure 3.5: (a) Relative momentum distributions and (b) two-pion correlation function for events with impact parameter $b = 0 - 4$ fm, computed from the MPD request 31 data.

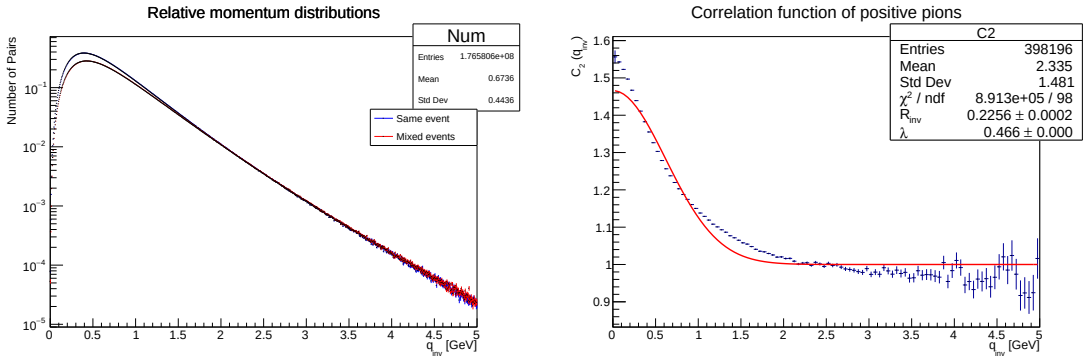

(a) Relative momentum distributions

(b) Two-pion correlation function

Figure 3.6: (a) Relative momentum distributions and (b) two-pion correlation function for events with impact parameter $b = 7 - 14$ fm, computed from the MPD request 31 data.

the correlation for relative momentum smaller than 250 MeV is above 2, which should not happen, since the maximum value that the correlation can take is 2. Also, for all the different impact parameter intervals, the width of the correlation function is about 1 GeV, which by Heisenberg uncertainty's principle is related to a source size of about 0.2 fm. This is in agreement with the radii obtained by the fit to a Gaussian function. However, the expected source size must be of about 5 fm, and hence, the source is about 25 times smaller than it should be.

Chapter 4

Conclusions

In this work, the two-pion correlation function was computed from real data of the 3.2 GeV argon run of the BM@N experiment and from pure Monte Carlo data of the request 31, which consists of bismuth - bismuth nuclei collisions at center of mass energy of $\sqrt{s_{NN}} = 9.2$ GeV.

The obtained results for the BM@N data showed no sign of correlation, possibly due to the extremely low statistics that is available in the data set. This problem could be solved by adding the data of the other part of the ToF400 detector that was not available for its analysis, as well as the inclusion of more data from other experimental runs.

On the other hand, the results for the MPD data did showed a correlation, however, the width of the correlation (and hence the inverse of the source radius) is extremely large, about 25 times larger than expected. During this internship, no explanation could be found on this issue. Since this is a work in progress, it is expected to be solved in the near future, as well as the developing of the analysis train of `mpdroot`, to include the simulated and reconstructed data on this analysis.

Nonetheless, the method for computing the two-pion correlation function was shown to work and to be an efficient one. There is a need for more statistics for an improvement of the results in the case of the BM@N data and a need to clarify what is the reason for the source size to be that small in the MPD data. Both needs imply that there should be more work done in both data sets. This work will be done in the near future.

Bibliography

[1] W. Greiner, *Quantum mechanics: Special chapters*, 1st ed. (Springer Berlin, Heidelberg, 1998).

[2] A. Ayala, S. Bernal-Langarica, and C. Villavicencio, "Finite volume and magnetic field effects on the two-pion correlation function in relativistic heavy-ion collisions," Phys. Rev. D **105**, 056001 (2022), arXiv:2111.05951 [hep-ph] .

[3] M. A. Lisa, S. Pratt, R. Soltz, and U. Wiedemann, "Femtoscopy in relativistic heavy ion collisions," Ann. Rev. Nucl. Part. Sci. **55**, 357–402 (2005), arXiv:nucl-ex/0505014 .

[4] H. Adhikary *et al.* (NA61/SHINE), "Measurements of two-pion HBT correlations in Be+Be collisions at 150A GeV/c beam momentum, at the NA61/SHINE experiment at CERN," (2023), arXiv:2302.04593 [nucl-ex] .

[5] S. Afanasiev *et al.* (BM@N), "Production of π^+ and K^+ mesons in argon-nucleus interactions at 3.2 A GeV," JHEP **07**, 174 (2023), arXiv:2303.16243 [hep-ex] .

[6] K. Alishina, V. Plotnikov, L. Kovachev, Y. Petukhov, and M. Rumyantsev, "Charged Particle Identification by the Time-of-Flight Method in the BM@N Experiment," Phys. Part. Nucl. **53**, 470–475 (2022).

[7] V. Abgaryan *et al.* (MPD), "Status and initial physics performance studies of the MPD experiment at NICA," Eur. Phys. J. A **58**, 140 (2022), arXiv:2202.08970 [physics.ins-det] .